Aquarius brightness temperature variations at Dome C and snow metamorphism at the surface

Ludovic Brucker[1,2], Emmanuel Dinnat[1,3], Ghislain Picard[4], and Nicolas Champollion[4]

[1] NASA GSFC Cryospheric Sciences Lab., code 615, Greenbelt, MD, USA
[2] Universities Space Research Association – GESTAR
[3] Chapman University, Orange, CA, USA
[4] Uni. Grenoble Alpes/CNRS, LGGE, Grenoble, France

Motivations

The Antarctic ice sheet is both an **actor** in the climate system and an **indicator** of its evolution

Ice sheet area $\sim 14.10^6$ km^2

Antarctica contains $\sim 90\%$ of total ice on Earth

Number of Automatic Weather Station ~ 100

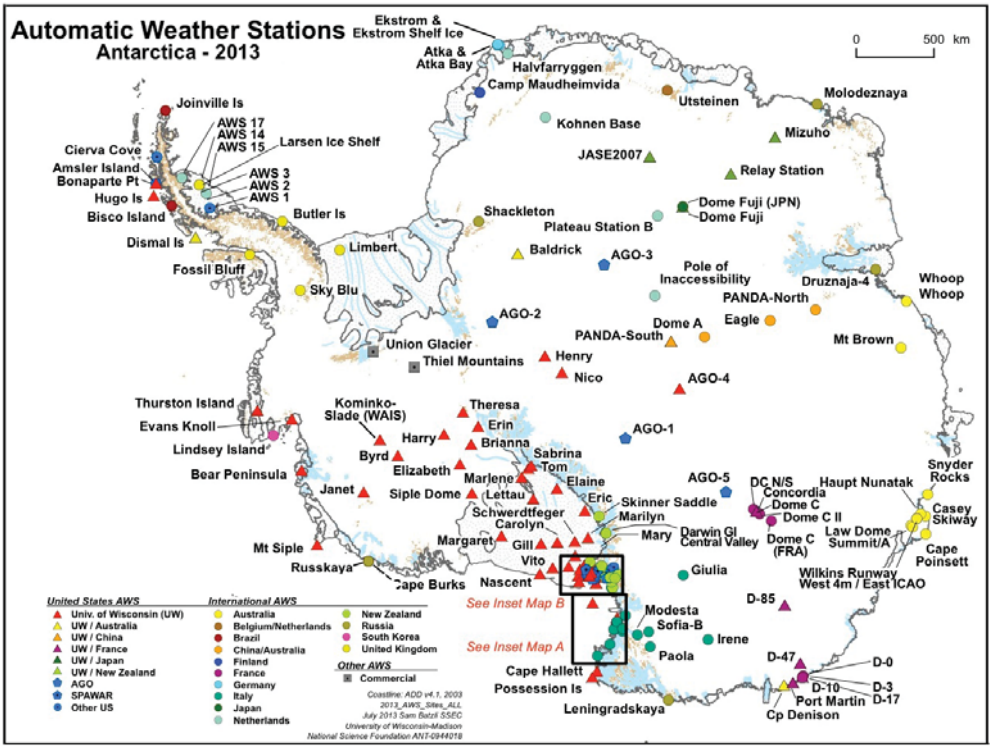

Motivations

The Antarctic ice sheet is both an **actor** in the climate system and an **indicator** of its evolution

Ice sheet area $\sim 14.10^6$ km^2

Antarctica contains $\sim 90\%$ of total ice on Earth

Number of Automatic Weather Station ~ 100

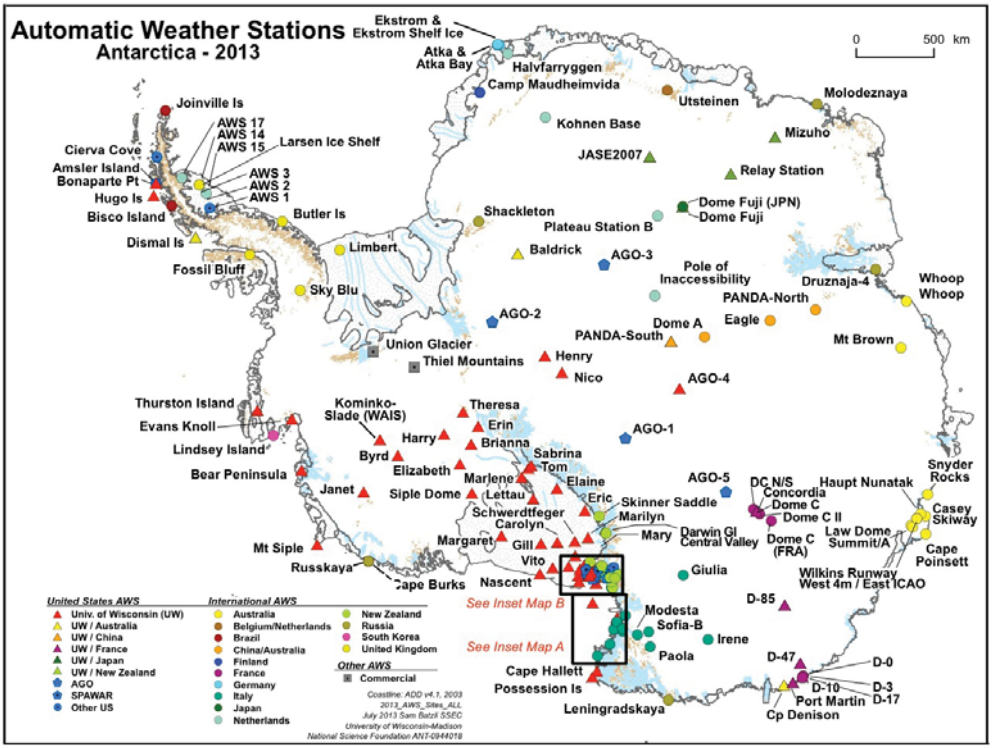

How to monitor ice temperature?

$\Rightarrow$ climate models (global, or regional)

$\Rightarrow$ reanalysis (ERA-interim, MERRA...)

$\Rightarrow$ remote sensing

Motivations

Motivated by L-band deep-penetration observations over Antarctica to:

- Analyze their spatial distribution
- Assess the observations' stability
- Contribute to define cal/val and intercalibration experiments

Important initial tasks toward retrieving snow & ice properties

The current 1.4 GHz (L-band) space-borne radiometers

Aquarius

SMOS

The current 1.4 GHz (L-band) space-borne radiometers

Aquarius

Designed for sea surface salinity retrievals
Operates **3** non-scanning radiometers

Radiometer	1	2	3
Incidence angle (^{o})	29.2	38.4	46.3
Footprint size (km$\times$km)	76$\times$94	84$\times$120	97$\times$156
Northernmost latitude (^{o})	84.99	86.07	87.40
Southernmost latitude (^{o})	79.01	77.90	76.54

Large footprint sizes, but
Excellent sensitivity of **0.2 K**

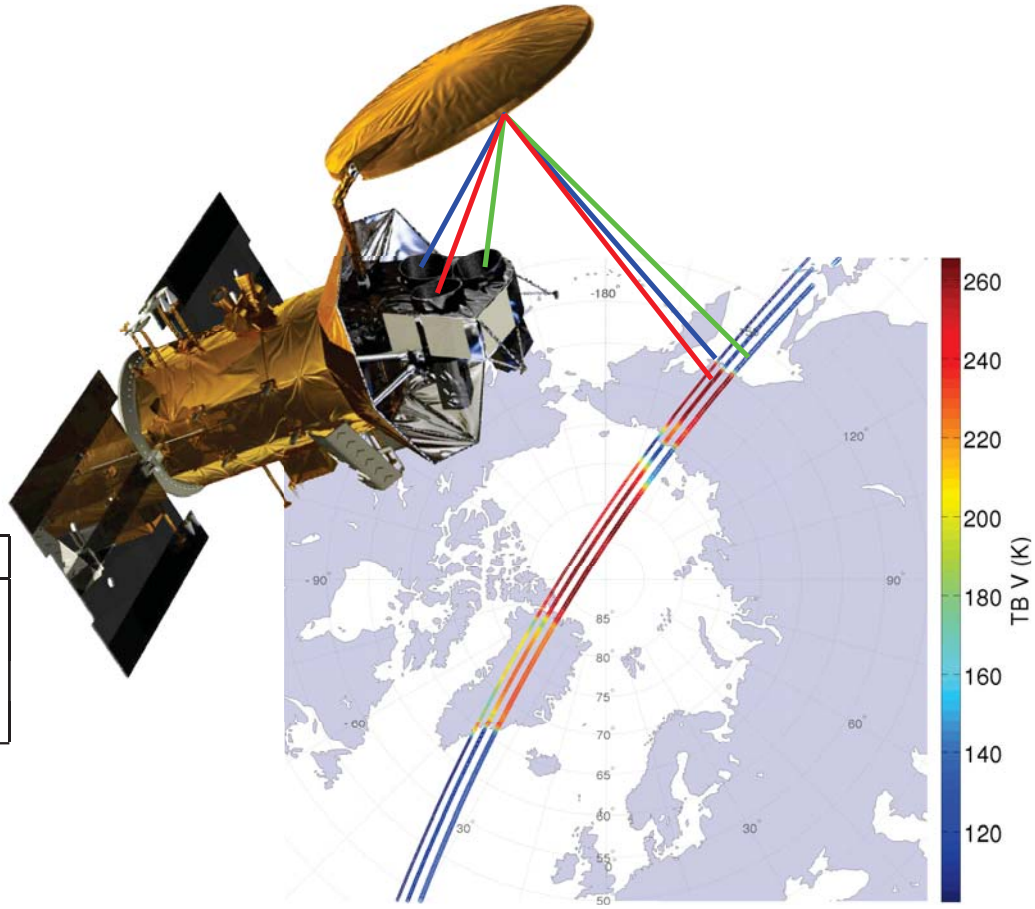

The current 1.4 GHz (L-band) space-borne radiometers

Aquarius

Designed for sea surface salinity retrievals
Operates **3** non-scanning radiometers

Radiometer	1	2	3
Incidence angle (^{o})	29.2	38.4	46.3
Footprint size (km$\times$km)	76$\times$94	84$\times$120	97$\times$156
Northernmost latitude (^{o})	84.99	86.07	87.40
Southernmost latitude (^{o})	79.01	77.90	76.54

Large footprint sizes, but
Excellent sensitivity of **0.2 K**

SMOS

Designed for moisture & salinity
Radiometer with aperture synthesis

Multiple incidence angles (0–65^{o})

Finer spatial resolution (30–90 km)
Coarser sensitivity (2–2.5 K)

Outline

Antarctica

Weekly mean brightness temperature (vertical polarization, radiometer 3 $\theta_{\mathrm{inc}} \sim 46.3^{\circ}$)

Winter

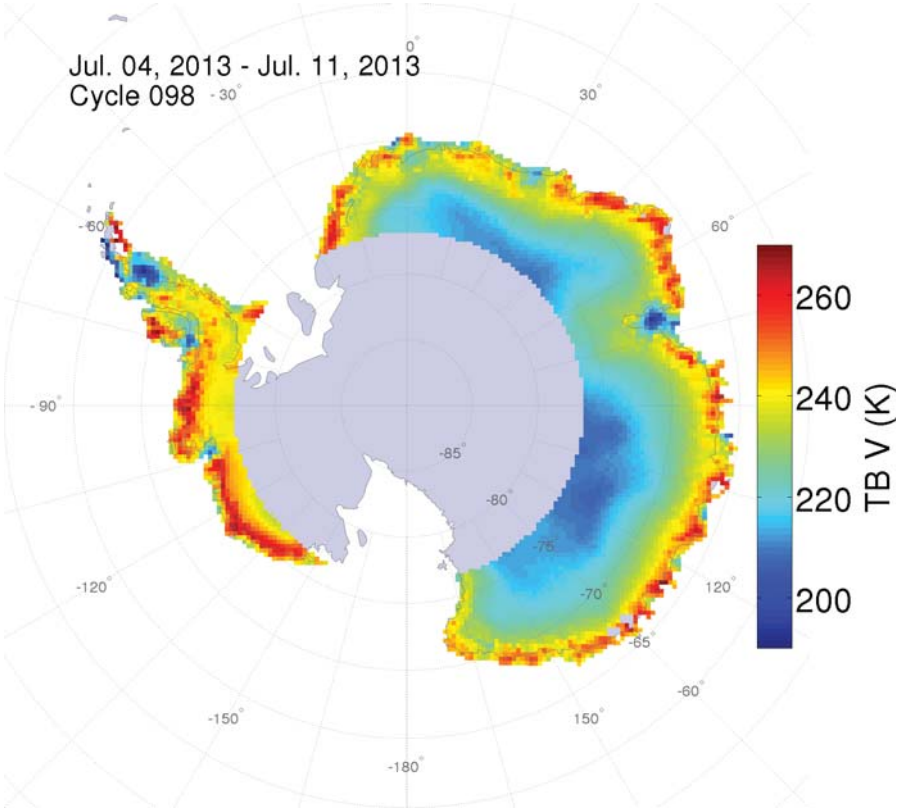

Summer

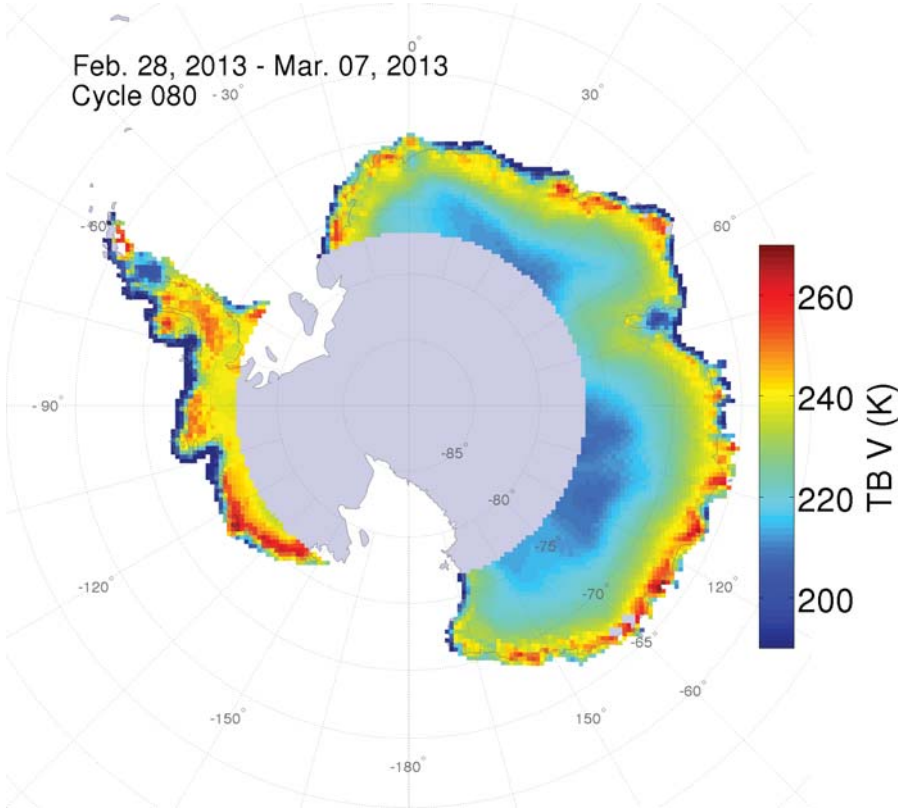

Coastal open water/sea ice modifies Aquarius TB

(Brucker et al., 2014 TC)

East Antarctica

Annual mean and standard deviation TB (radiometer 1, $\theta_{\mathrm{inc}} \sim 29.2^{\mathrm{o}}$)

TB V

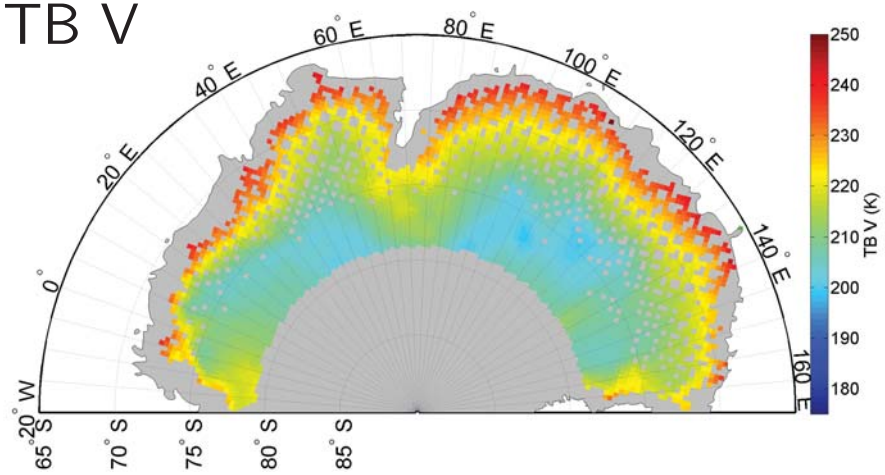

TB H

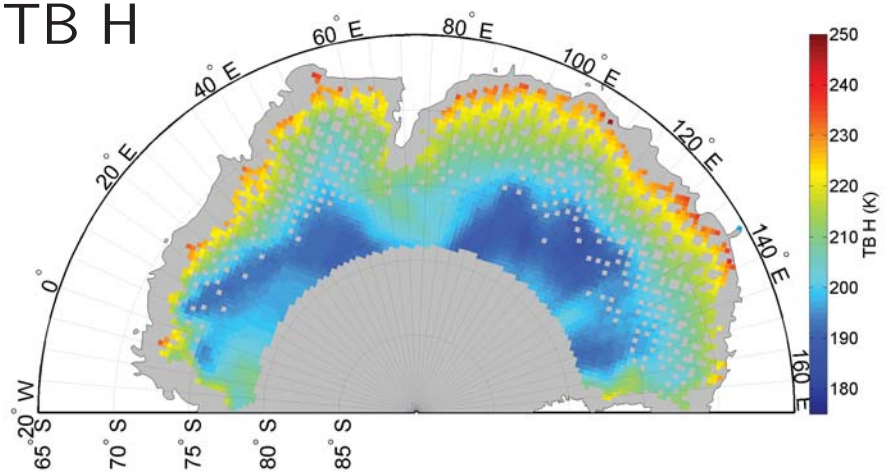

Stdev TB V

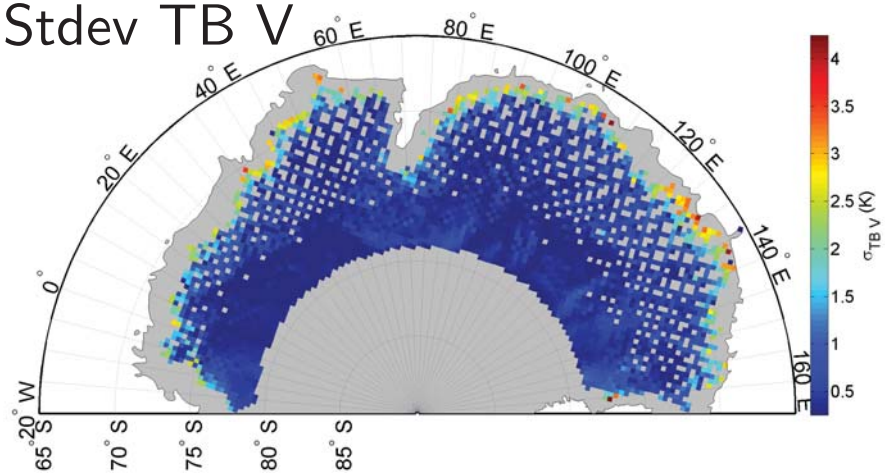

Stdev TB H

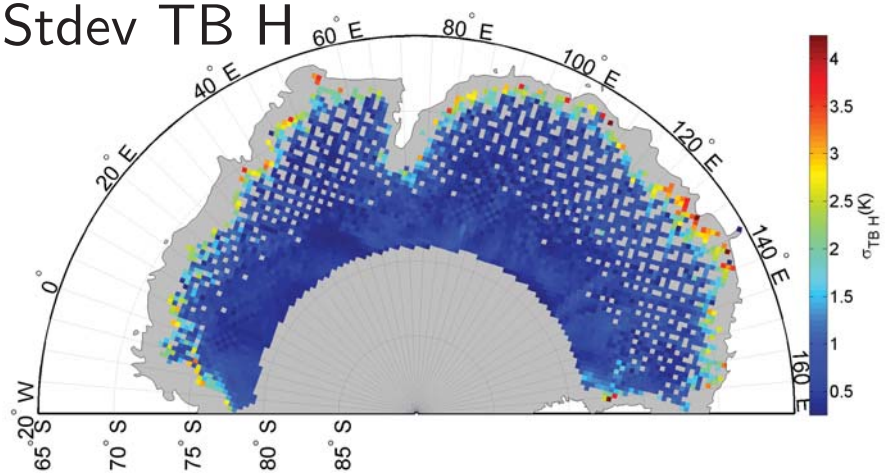

Areas where melt events occurred since August 1, 2000 were masked.
There are grid cells (36 km) without observations.

Dome C, Antarctic Plateau (3240 m)

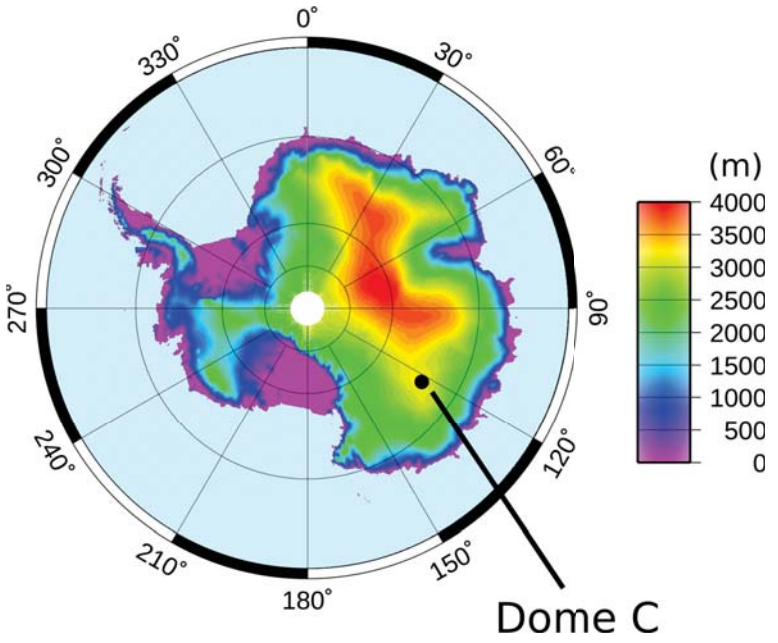

Snow temperature below 15 m:
218.42±0.07 K *(Brucker et al., 2011)*

Snow accumulation:
8–10 cm of snow *(Urbini et al., 2008)*

Ideal site to study the relationship: microwave observations – ice properties

Dome C – TB timeseries

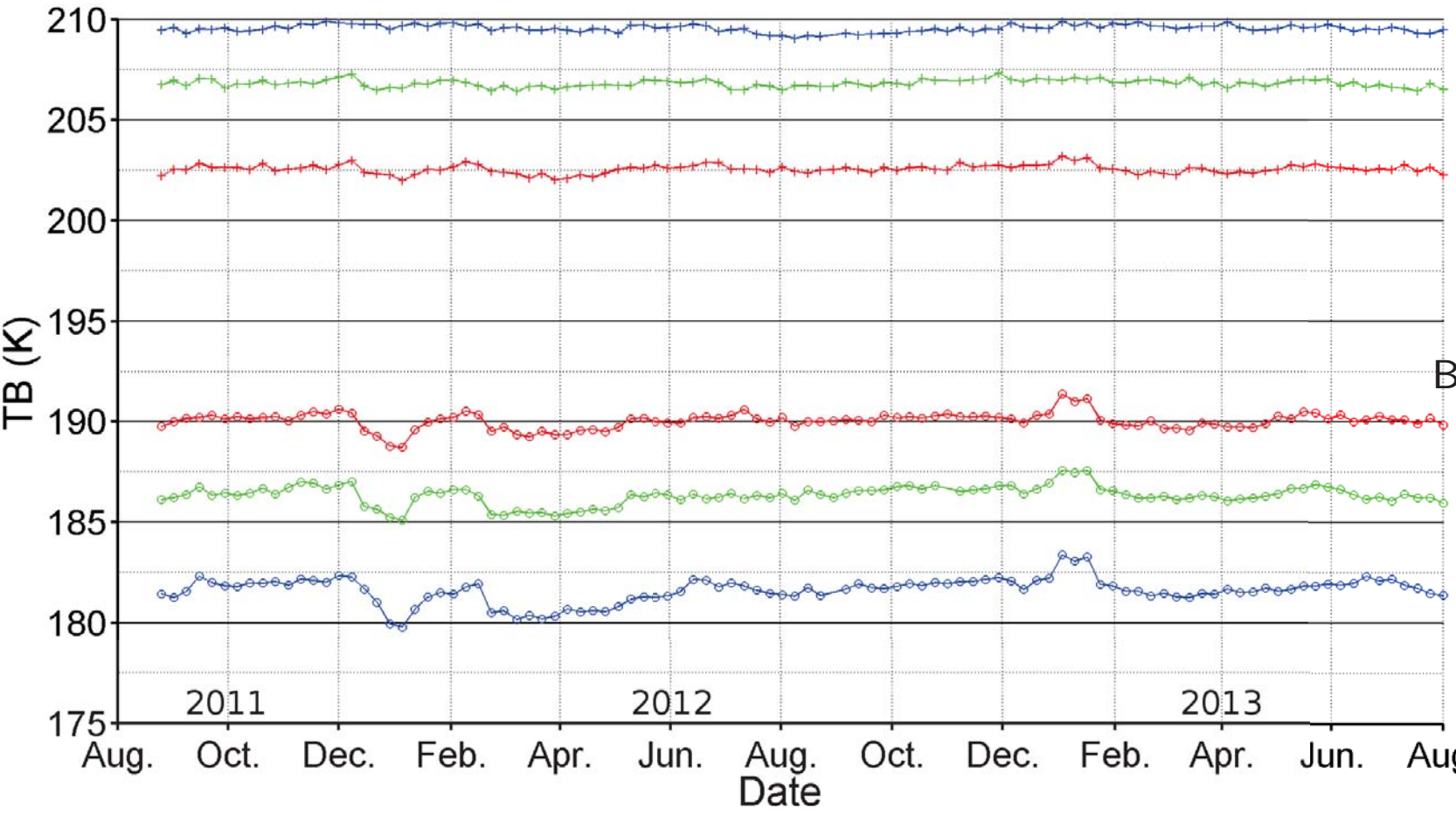

Beam	TB V (K)
3	209.50±0.26
2	206.79±0.25
1	202.54±0.28

Beam	TB H (K)
1	189.97±0.44
2	186.22±0.53
3	181.39±0.72

Sensitivity ∼0.2 K

Dome C – TB angular diagram

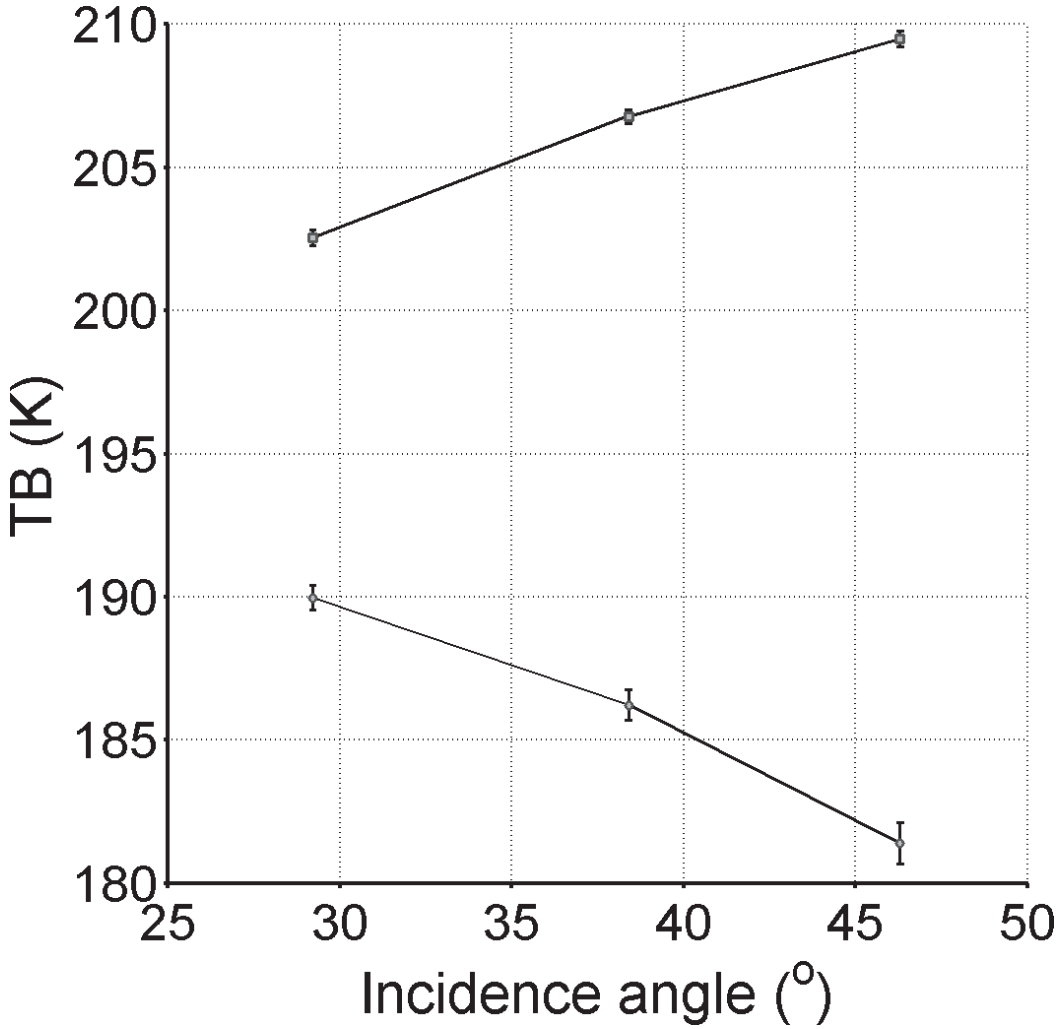

Beam	TB V (K)
3	209.50±0.26
2	206.79±0.25
1	202.54±0.28

Beam	TB H (K)
1	189.97±0.44
2	186.22±0.53
3	181.39±0.72

Sensitivity ∼0.2 K

Dome C – TB timeseries

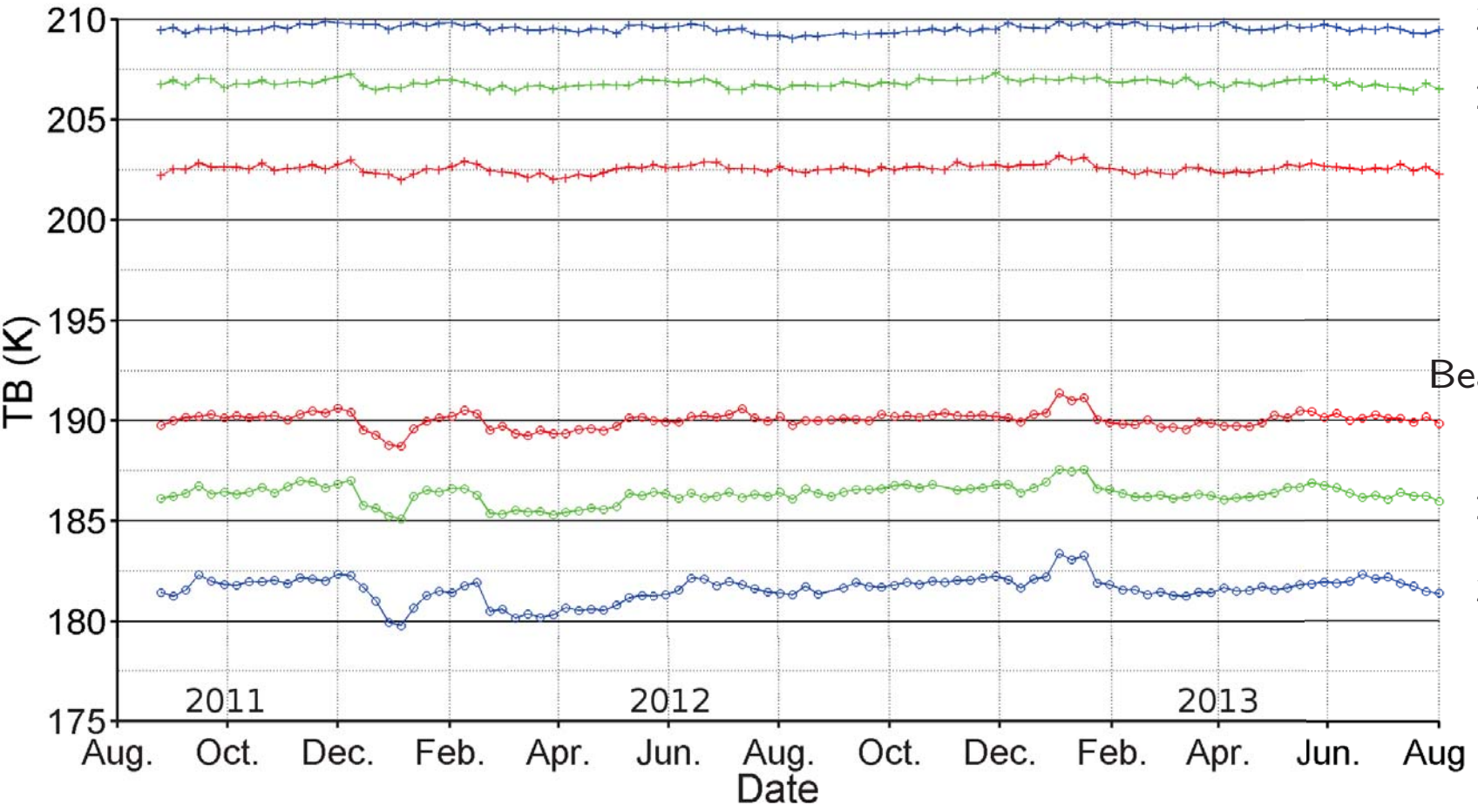

Beam	TB V (K)
3	209.50±0.26
2	206.79±0.25
1	202.54±0.28

Beam	TB H (K)
1	189.97±0.44
2	186.22±0.53
3	181.39±0.72

Sensitivity ∼0.2 K

Fast variations ⇝ surface changes?

Dome C – TB H/V timeseries

Focus on $\frac{TB_H}{TB_V}$. removes the dependency on the physical temperature
. highlights emissivity variations

Dome C – TB H/V timeseries

Focus on $\frac{TB_H}{TB_V}$. removes the dependency on the physical temperature
. highlights emissivity variations

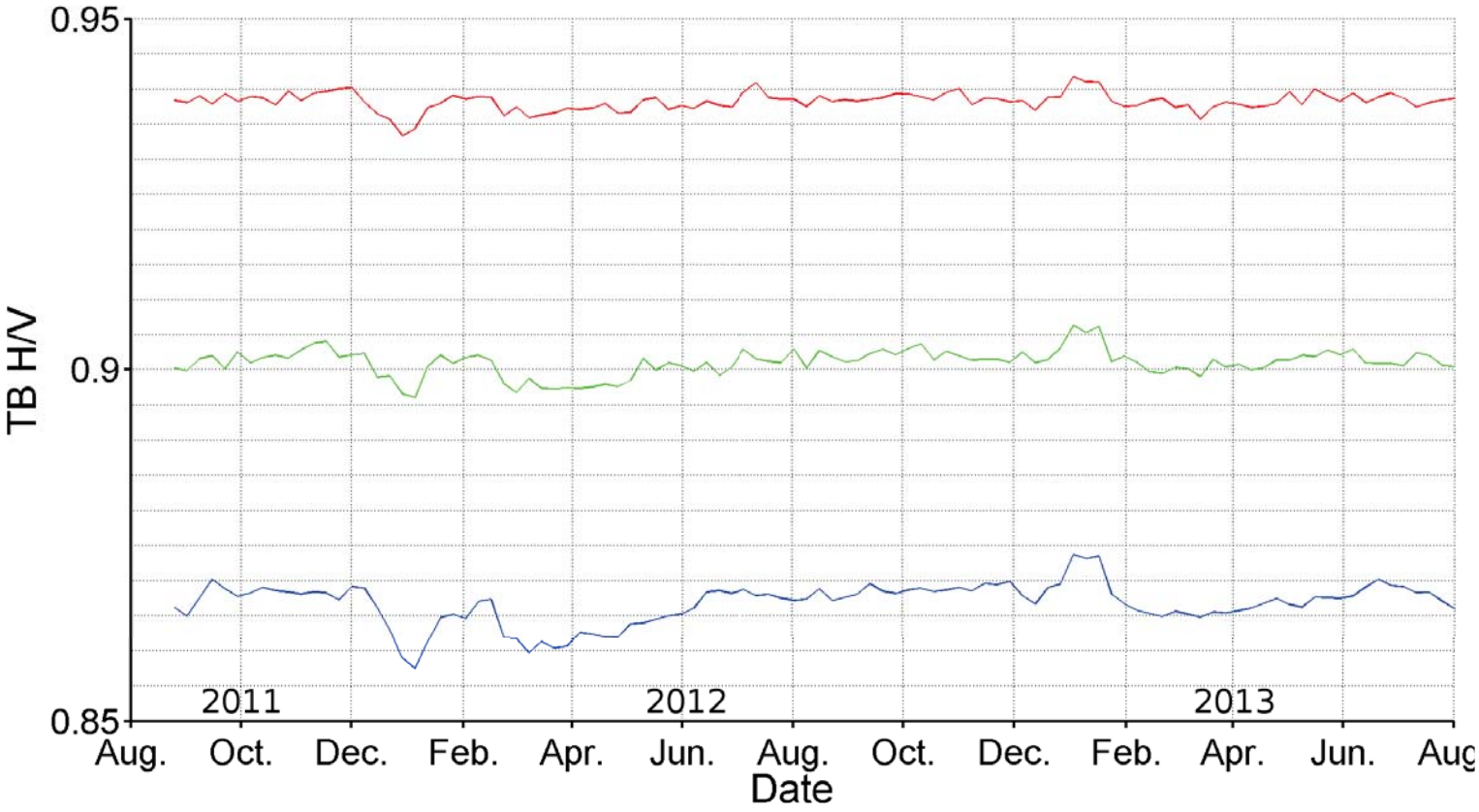

Radiometer 1
($\theta_{\text{inc}} \sim 29.2^{\text{o}}$)

Radiometer 2
($\theta_{\text{inc}} \sim 38.4^{\text{o}}$)

Radiometer 3
($\theta_{\text{inc}} \sim 46.3^{\text{o}}$)

Variation > 0.001 is above the radiometric noise
The largest variations are observed by radiometer 3

Satellite monitoring of the snow surface at Dome C

AMSU-B grain index derived from AMSU-B *(Picard et al., 2012)*,

$$\mathrm{GI} = 1 - \frac{\mathrm{TB150}}{\mathrm{TB89}}$$

with shallow penetration (few cm) channels

Satellite monitoring of the snow surface at Dome C

AMSU-B grain index derived from AMSU-B *(Picard et al., 2012)*,

$$\mathrm{GI} = 1 - \frac{\mathrm{TB150}}{\mathrm{TB89}}$$

with shallow penetration (few cm) channels

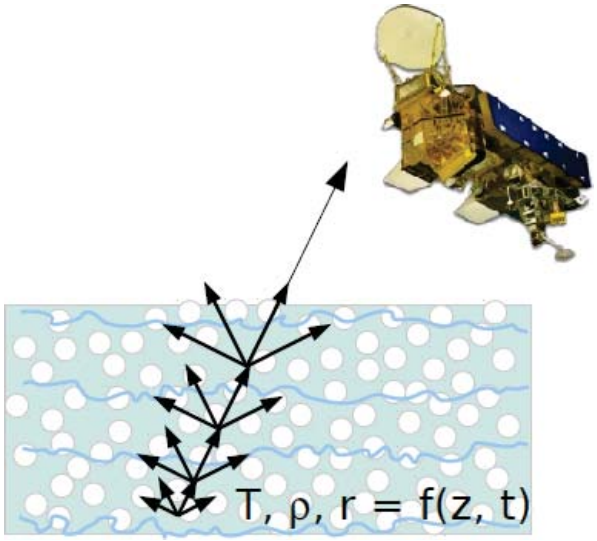

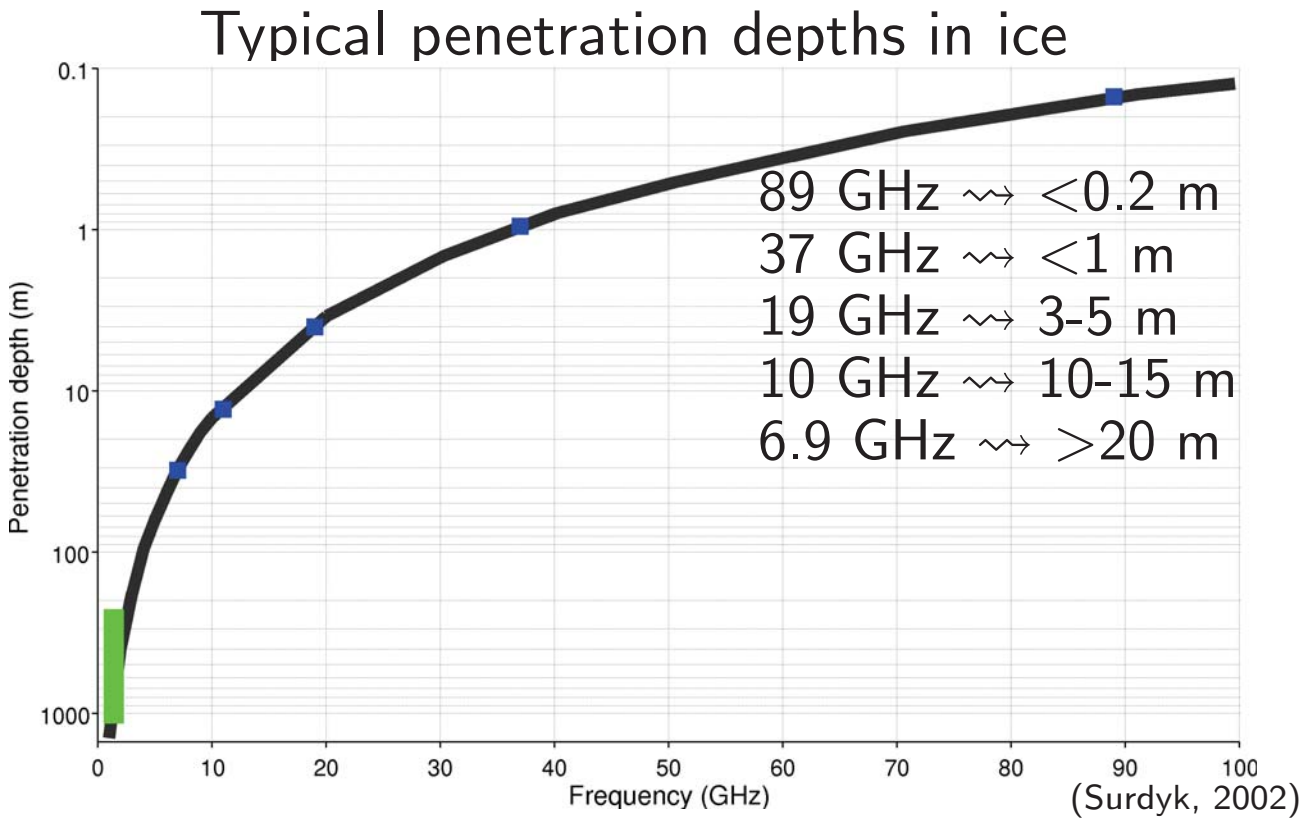

L-band observations have a large penetration in ice

Satellite monitoring of the snow surface at Dome C

AMSU-B grain index derived from AMSU-B *(Picard et al., 2012)*,

$$\mathrm{GI} = 1 - \frac{\mathrm{TB150}}{\mathrm{TB89}}$$

with shallow penetration (few cm) channels

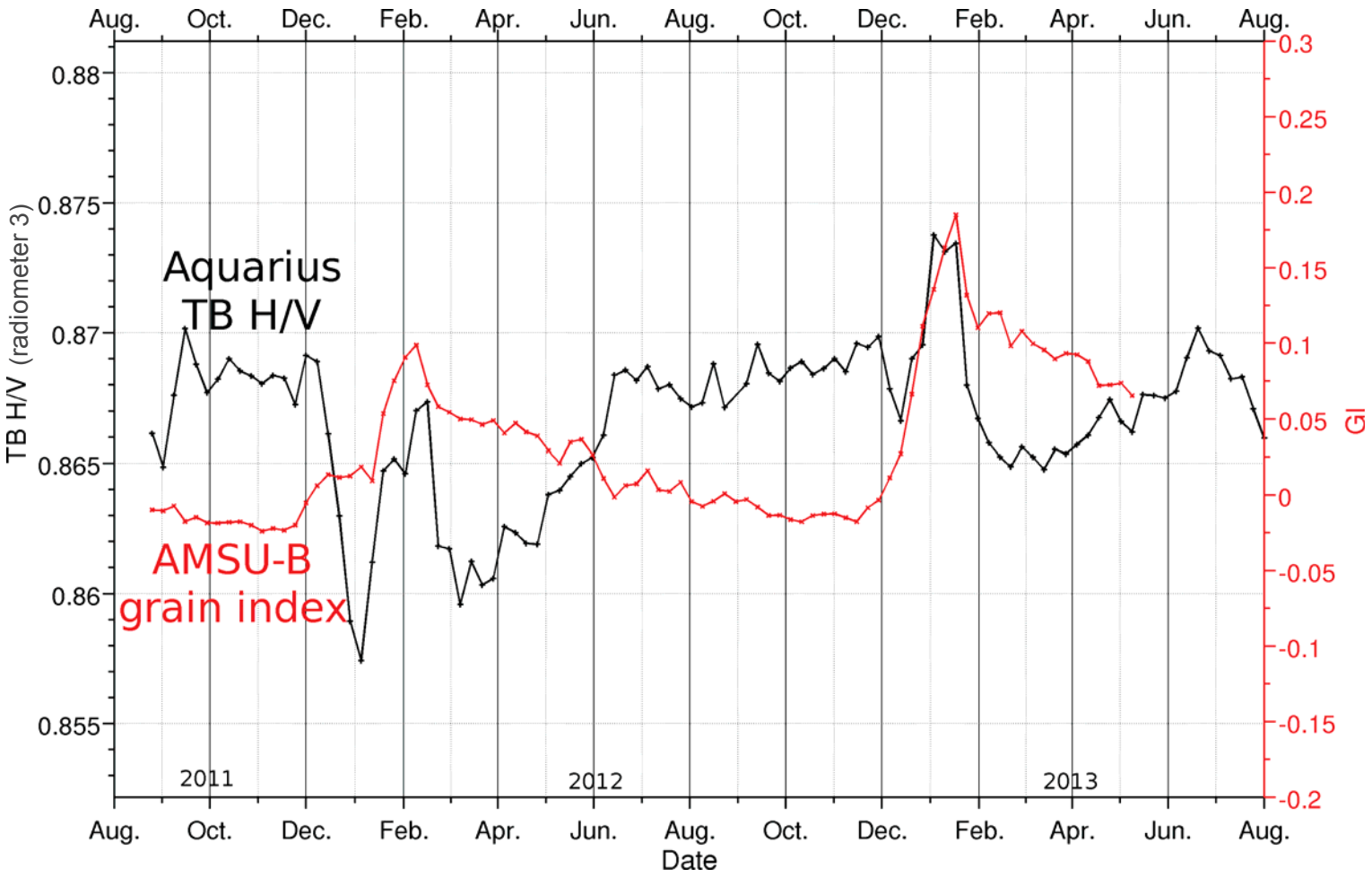

Good synchronization of the variations in summer

Surface-based monitoring of the snow surface at Dome C

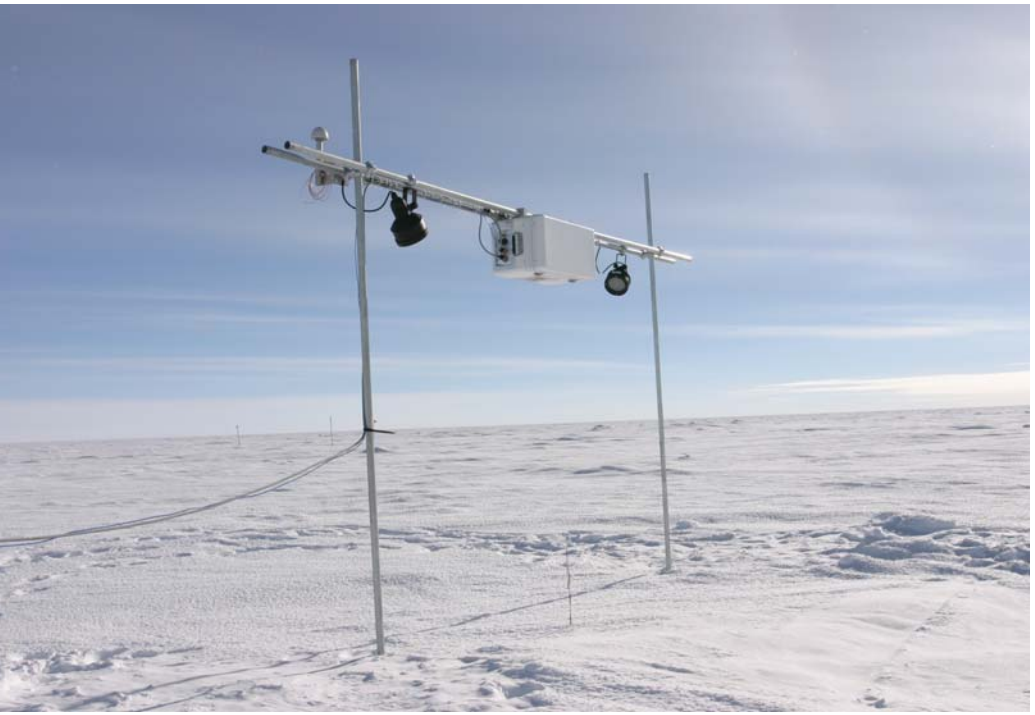

(Champollion et al., 2013)

Near IR camera
2 m high
imaged area $\sim$ 4 m^2

Surface-based monitoring of the snow surface at Dome C

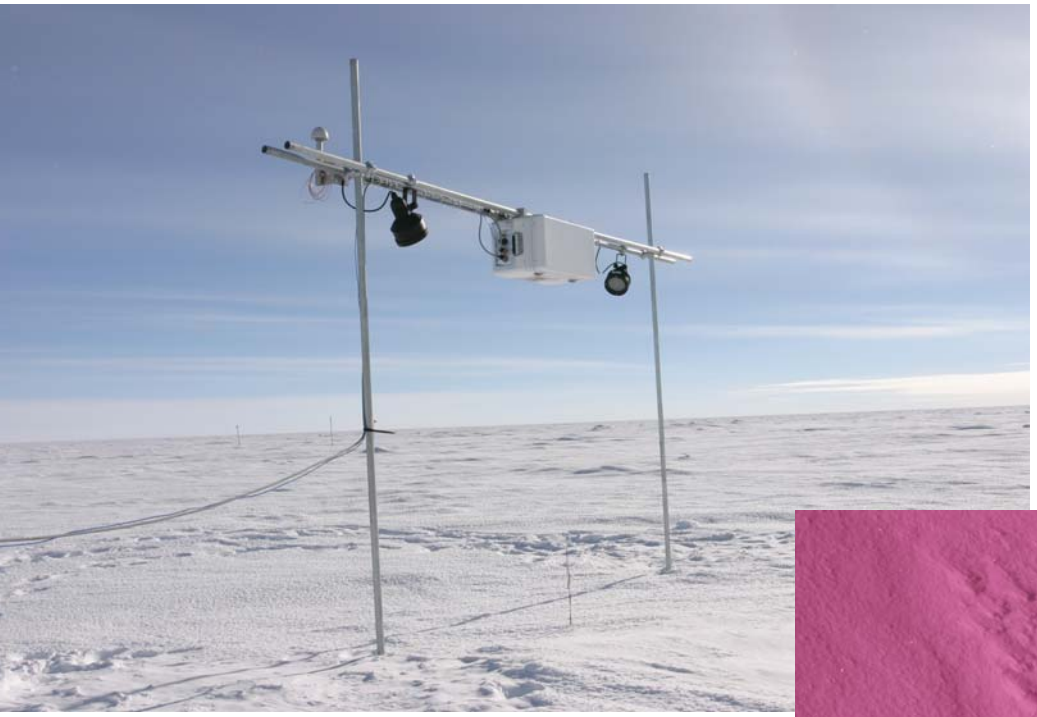

(Champollion et al., 2013)

Near IR camera
2 m high
imaged area $\sim$ 4 m^2

Surface-based monitoring of the snow surface at Dome C

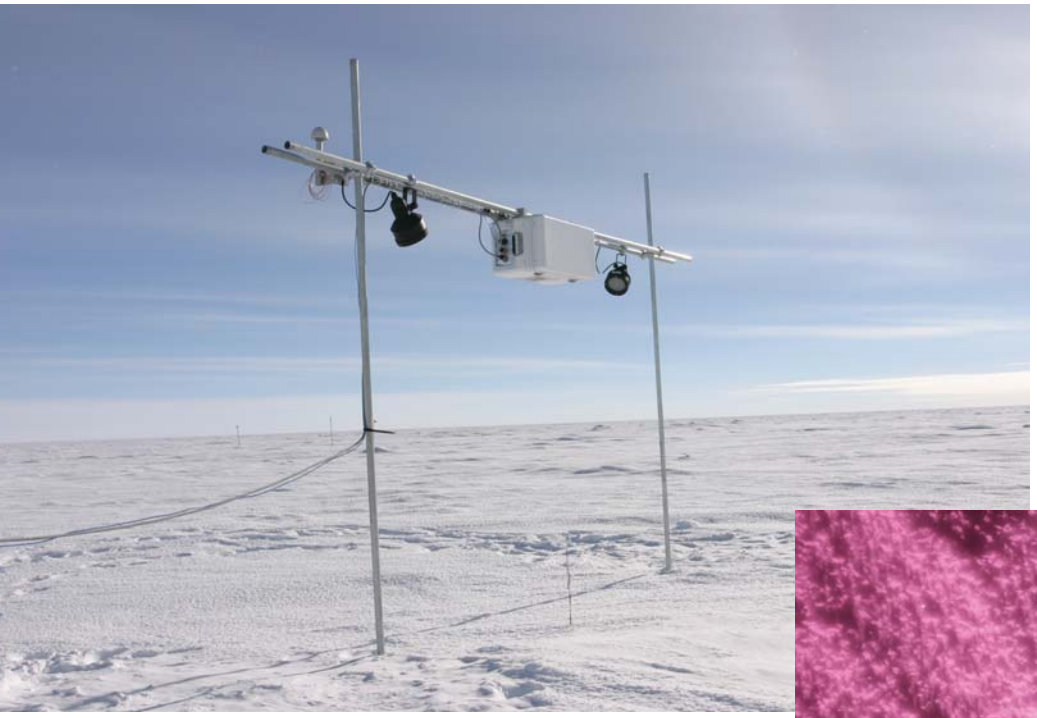

(Champollion et al., 2013)

Near IR camera
2 m high
imaged area $\sim$ 4 m^2

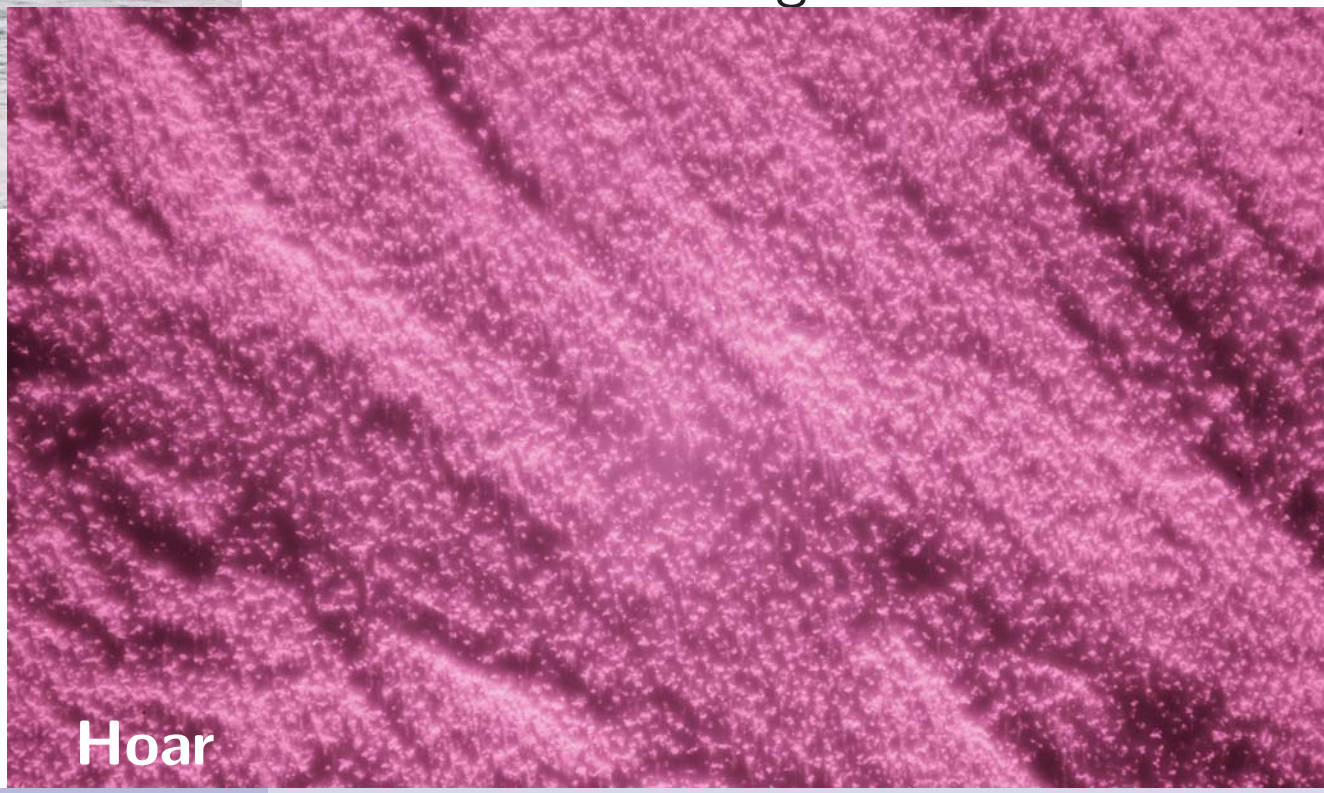

Surface-based monitoring of the snow surface at Dome C

(Champollion et al., 2013)

Near IR camera
2 m high
imaged area $\sim$ 4 m^2

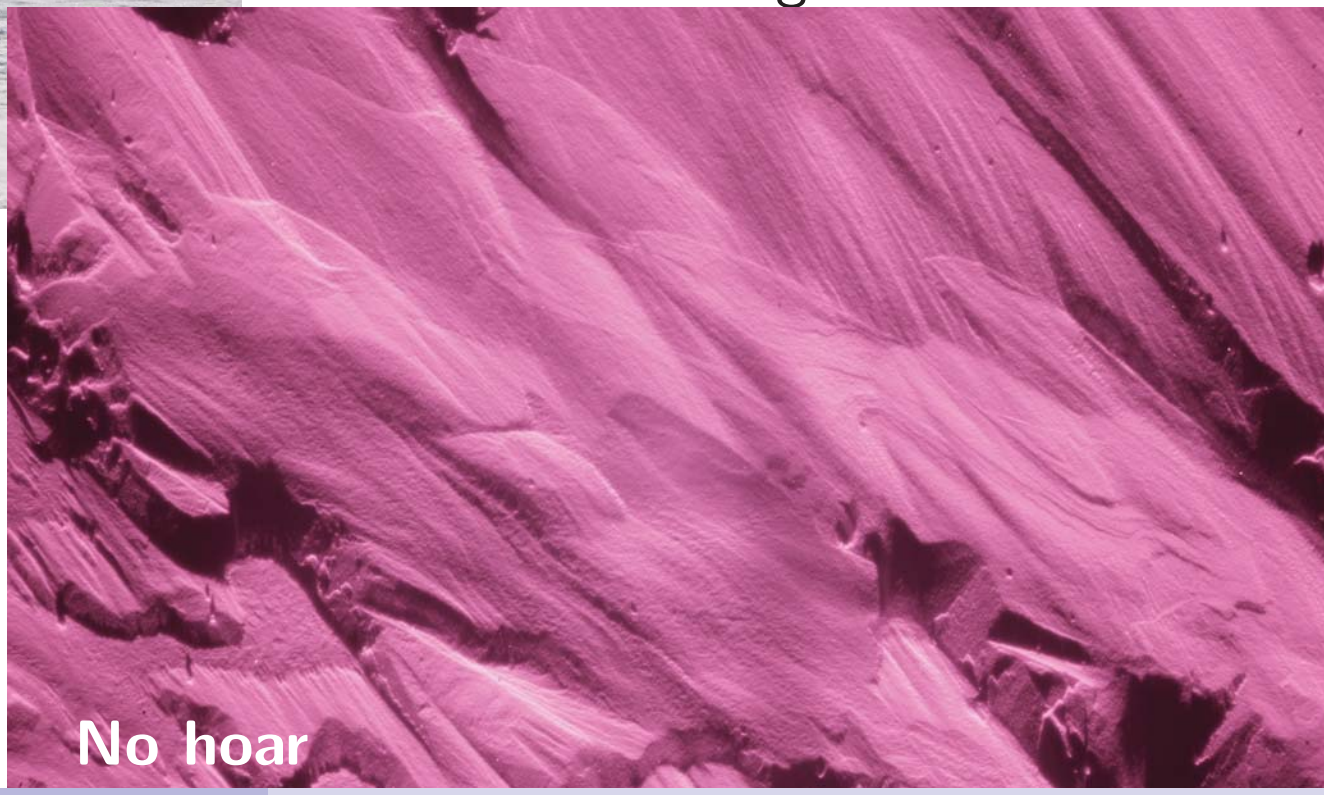

Surface-based monitoring of the snow surface at Dome C

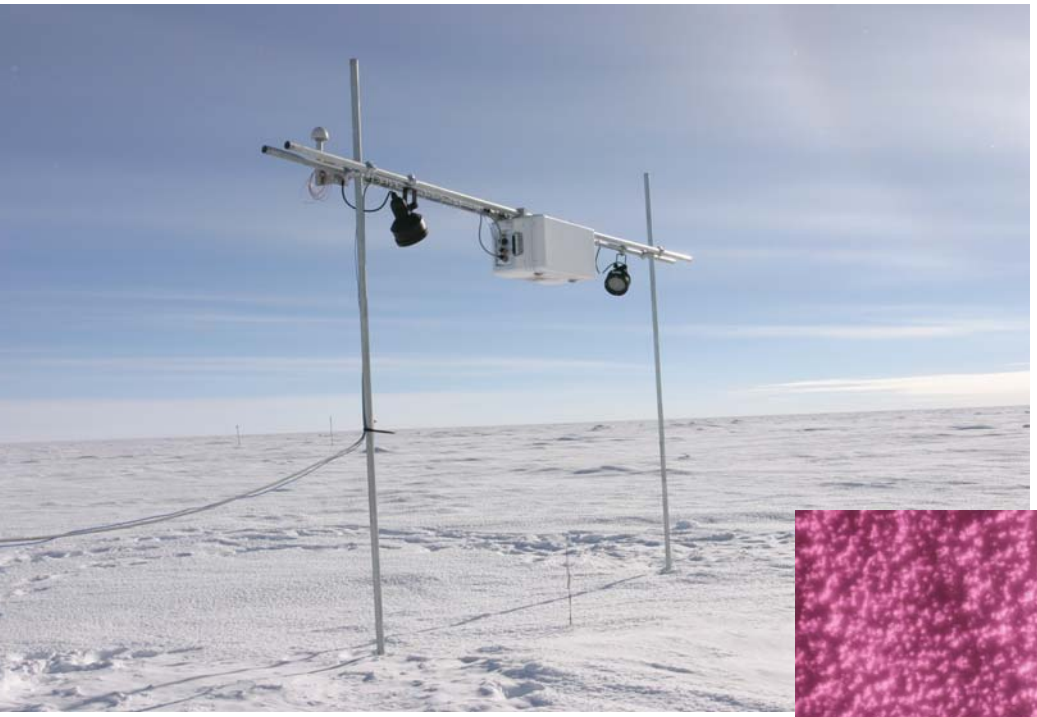

(Champollion et al., 2013)

Near IR camera
2 m high
imaged area $\sim$ 4 m^2

Aquarius and hoar crystal on the surface

No hoar Hoar

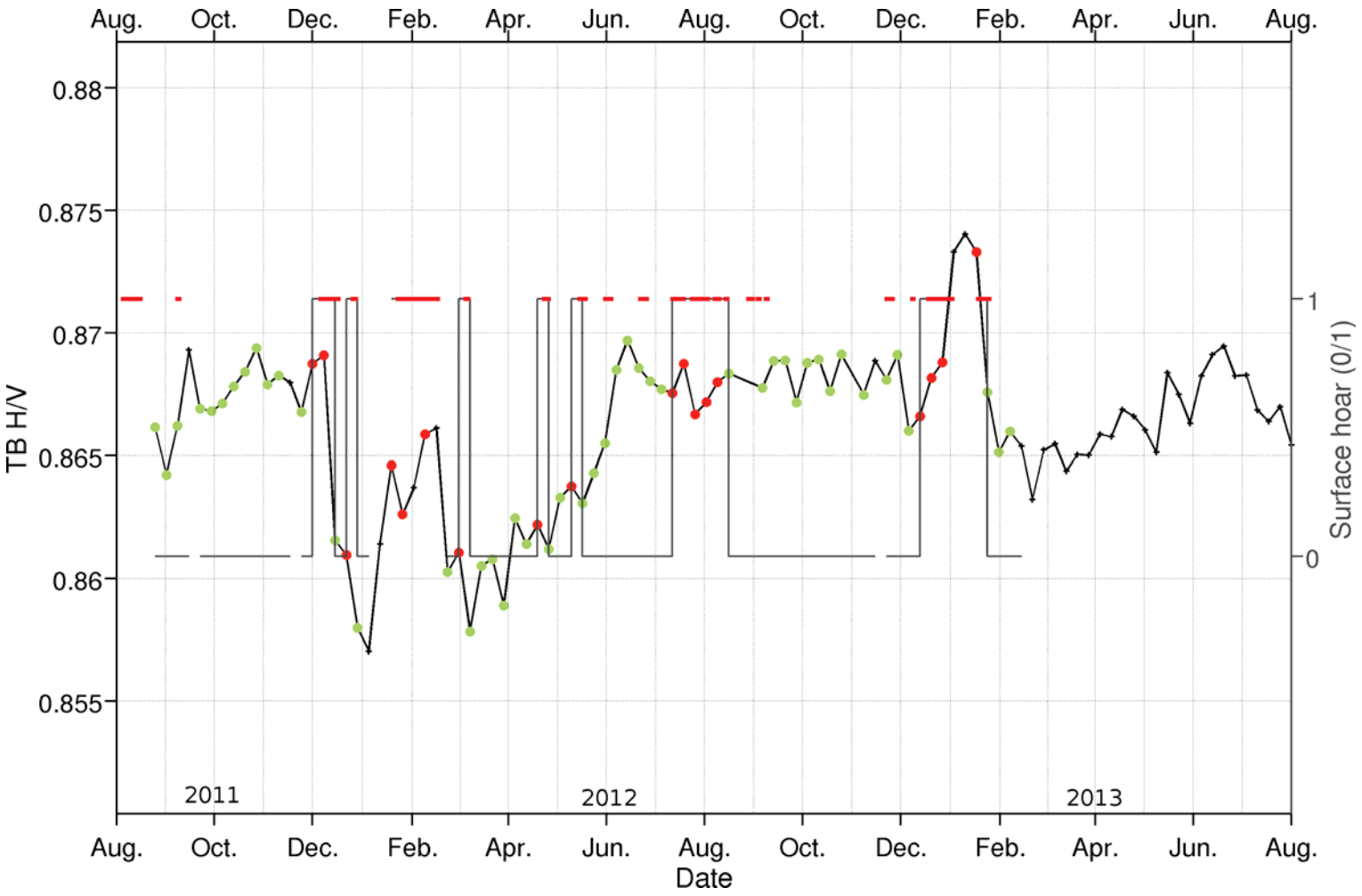

Aquarius and hoar crystal on the surface

No hoar Hoar

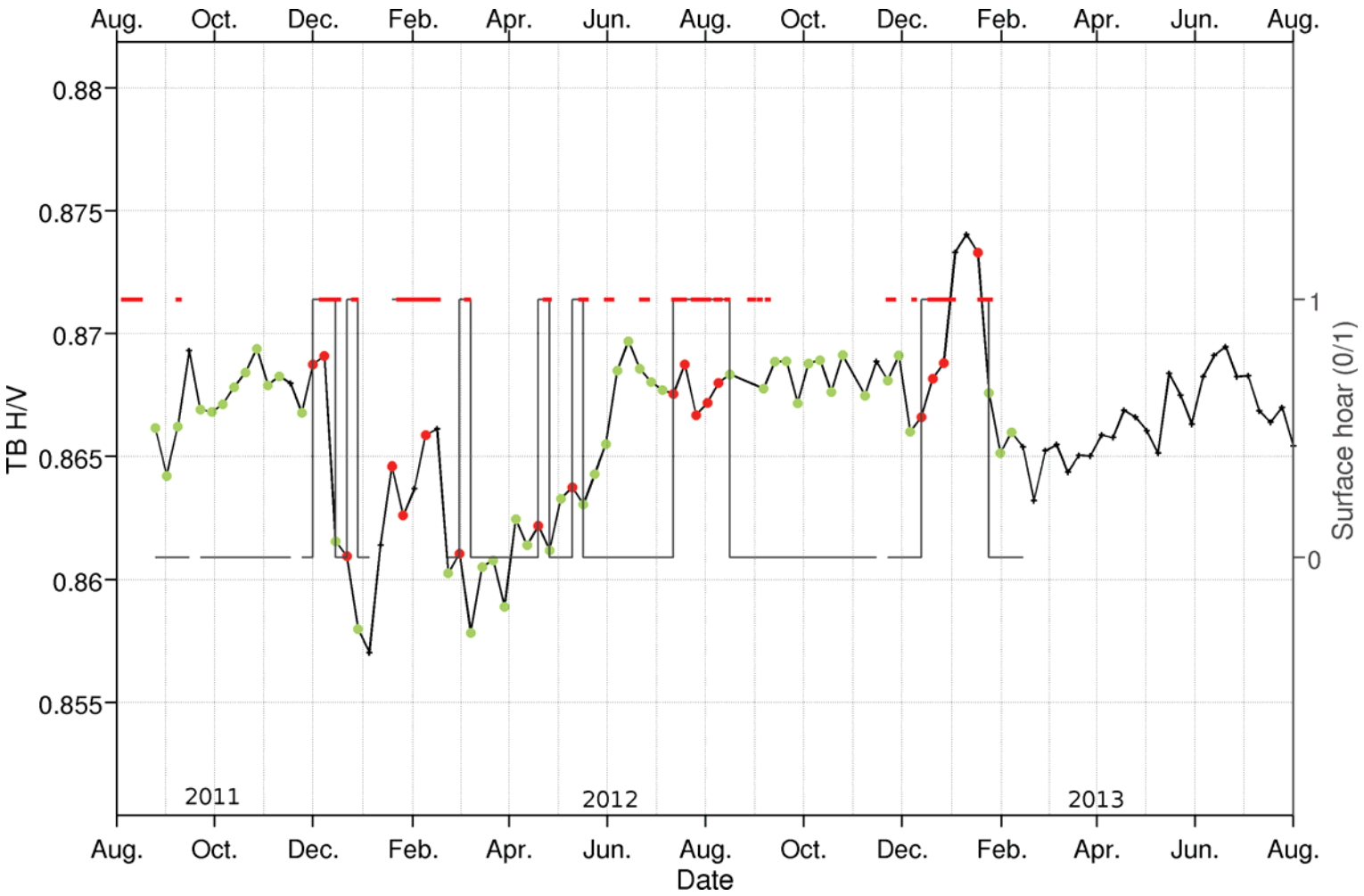

L-band observations are sensitive to surface snow properties

A simple calculation with Fresnel's reflection coefficients at the air/snow interface

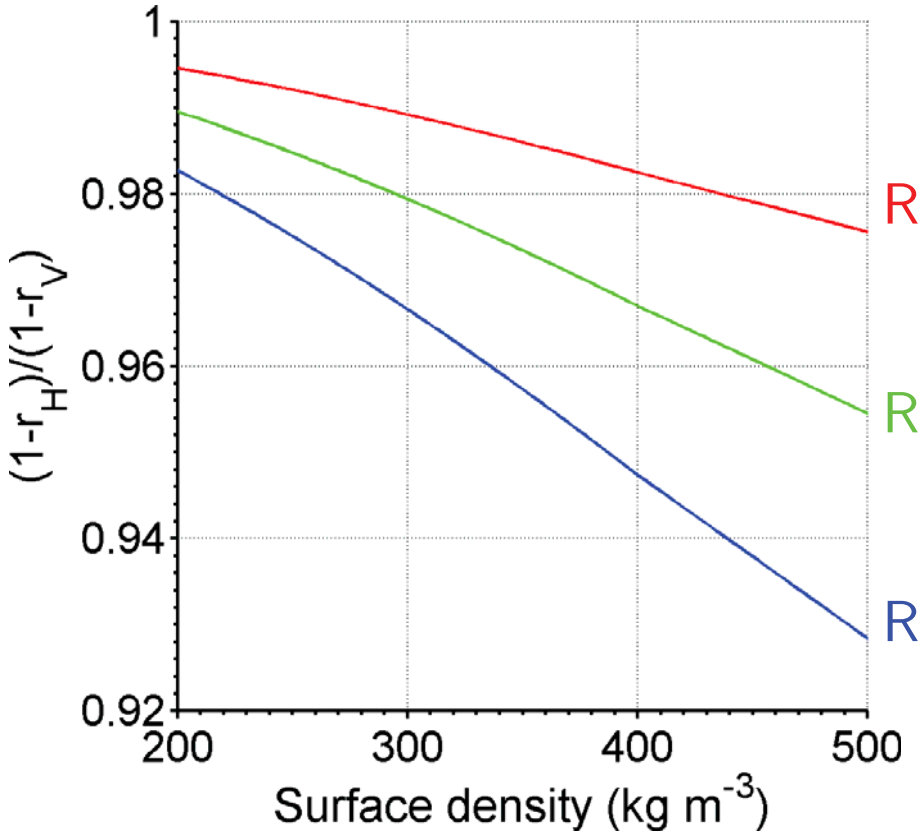

Radiometer 1 ($\theta_{\text{inc}} \sim 29.2°$)

Radiometer 2 ($\theta_{\text{inc}} \sim 38.4°$)

Radiometer 3 ($\theta_{\text{inc}} \sim 46.3°$)

A density variation of 75 kg m^{-3}
could explain the largest change in TB H/V (in Dec. 2011)

Conclusion

Aquarius radiometers . have an excellent sensitivity (0.2 K)
. are thus appealing to study the ice sheets

TB variability at H polarization . is larger than at V polarization
. increases as θ_{inc} increases
. is larger than the sensors' sensitivity

L-band radiation . has a deep penetration
. but is sensitive to surface snow properties

Hoar crystals on the surface may influence cal/val experiments

Brucker et al., 2014: Effect of Snow Surface Metamorphism on Aquarius L-Band Radiometer Observations at Dome C, Antarctica. IEEE TGRS 52(11): 7408-7417, doi:10.1109/TGRS.2014.2312102.

Dome C

Wind direction

Hoar crystals present

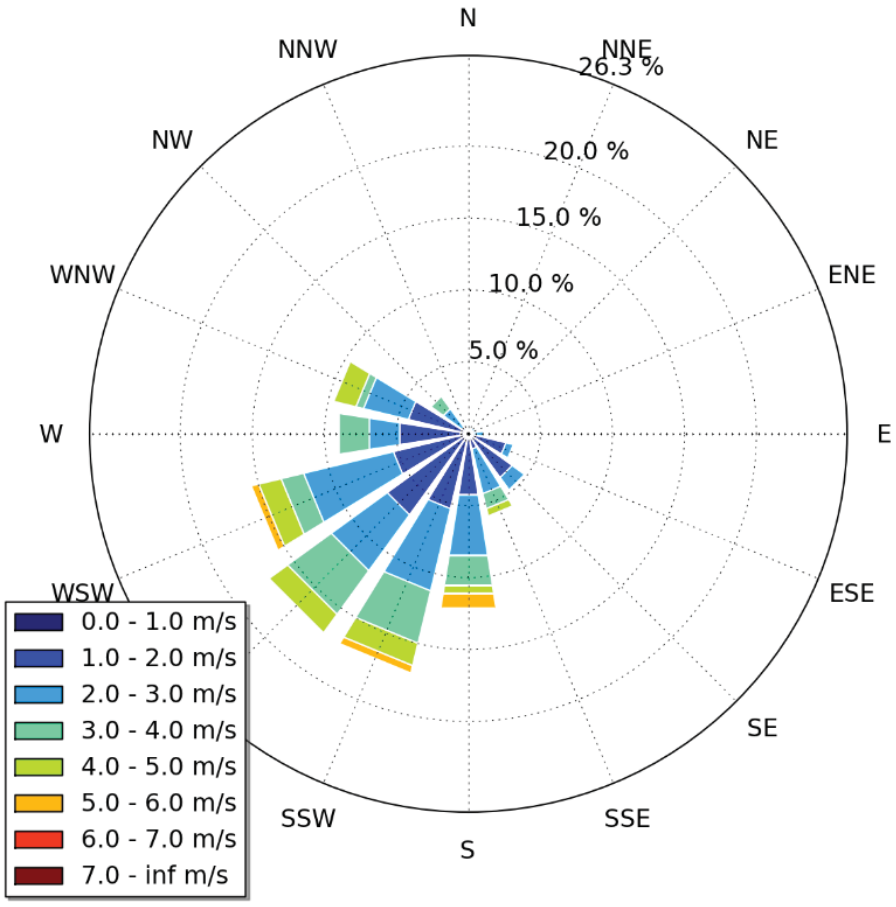

Hoar crystals disappear

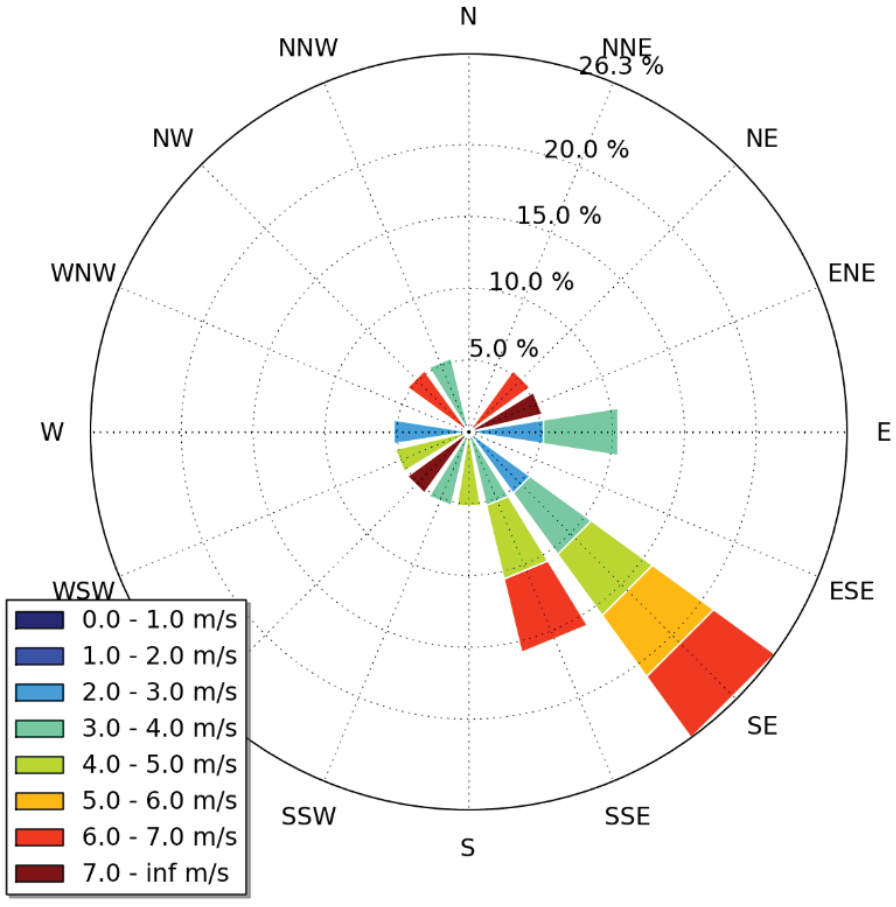

(Champollion et al., 2013)

See also: Gallet et al. (2014), The growth of sublimation crystals and surface hoar on the Antarctic plateau, The Cryosphere.